J Antimicrob Chemother 2021; **76**: 639–647
doi:10.1093/jac/dkaa471 Advance Access publication 13 November 2020

Journal of Antimicrobial Chemotherapy

Progressive emergence of an S153F plus R263K combination of integrase mutations in the proviral DNA of one individual successfully treated with dolutegravir

Hanh T. Pham[1,2]†, Brunna M. Alves[3]†, Sunbin Yoo[1,2], Meng A. Xiao[1,2], Jing Leng[1,2], Peter K. Quashie[4,5,6], Esmeralda A. Soares[3], Jean-Pierre Routy[7], Marcelo A. Soares[3,8] and Thibault Mesplède[1,2]*

[1]McGill AIDS Centre, Lady Davis Institute for Medical Research, Jewish General Hospital, Montréal, Québec, Canada; [2]Department of Microbiology and Immunology, Faculty of Medicine, McGill University, Montréal, Québec, Canada; [3]Programa de Oncovirologia, Instituto Nacional de Câncer, Rio de Janeiro, Brazil; [4]West African Centre for Cell Biology of Infectious Pathogens, University of Ghana, Accra, Ghana; [5]The Francis Crick Institute, London, UK; [6]Department of Virology, Noguchi Memorial Institute for Medical Research, University of Ghana, Accra, Ghana; [7]For Montreal PHI Cohort Study Group, Division of Hematology, McGill University Health Centre, Montréal, Québec, Canada; [8]Departamento de Genética, Universidade Federal do Rio de Janeiro, Rio de Janeiro, Brazil

*Corresponding author. E-mail: tibo_mes@hotmail.com
†Equal contribution.

Received 6 July 2020; accepted 19 October 2020

Objectives: The development of HIV drug resistance against the integrase strand transfer inhibitor dolutegravir is rare. We report here the transient detection, by near full-genome ultradeep sequencing, of minority HIV-1 subtype B variants bearing the S153F and R263K integrase substitutions in the proviral DNA from blood cells of one patient who successfully initiated dolutegravir-based ART, over 24 weeks. Our objective was to study the effects of these substitutions.

Methods: Strand transfer and DNA-binding activities of recombinant integrase proteins were measured in cell-free assays. Cell-based resistance, infectivity and replicative capacities were measured using molecular clones. Structural modelling was performed to understand experimental results.

Results: R263K emerged first, followed by the addition of S153F at Week 12. By Week 24, both mutations remained present, but at lower prevalence. We confirmed the coexistence of S153F and R263K on single viral genomes. Combining S153F or S153Y with R263K decreased integration and viral replicative capacity and conferred high levels of drug resistance against all integrase inhibitors. Alone, S153Y and S153F did little to infectivity or dolutegravir resistance. We identified altered DNA binding as a mechanism of resistance. The patient remained with undetectable viral loads at all timepoints.

Conclusions: Drug-resistant minority variants have often been reported under suppressive ART. Our study adds to these observations by unravelling a progression towards higher levels of resistance through a novel pathway despite continuous undetectable viral loads. Poorly replicative HIV drug-resistant minority proviral variants did not compromise viral suppression in one individual treated with dolutegravir.

Introduction

Highly active ART (HAART) is the standard of care to treat HIV infections. HAART regimens combine either two or three antiretroviral drugs to limit the development of drug resistance associated with single-agent therapy. Generally recommended initial treatment regimens typically include one integrase strand transfer inhibitor (INSTI).[1] Four members of this drug class are clinically approved for the treatment of HIV infection in adults: raltegravir, elvitegravir, dolutegravir and bictegravir.[2,3] A fifth INSTI called cabotegravir has been approved in Canada. Similar to other antiretroviral drugs,[4] INSTIs are susceptible to the development of HIV drug resistance mutations associated with treatment failure.[5] Treatment failure with emerging resistance mutations necessitates switching to alternative treatment regimens, which can be more expensive and cumbersome to patients. Treatment switch following the development of HIV drug resistance can also complicate the avoidance of drug–drug interactions, particularly in polymedicated individuals such as older HIV-positive individuals. Dolutegravir has a high barrier against the development of resistance when it is used as first-line therapy in combination with two active reverse transcriptase

inhibitors.[6,7] When dolutegravir is used either in patients who have previously experienced treatment failure or as a single antiretroviral agent, it is susceptible to the development of drug resistance mutations in integrase, including R263K, S230R, G118R and N155H.[8–18] Bictegravir is another antiretroviral drug that is robust against the development of drug resistance after treatment failure.[3]

The S153Y substitution in integrase has been selected either alone or in combination with T66I during cell-based selection experiments with the L-708,906, L-731,988 and L-841,411 preclinical INSTIs.[19,20] Addition of S153Y to T66I was later confirmed to increase resistance levels against diketo acid-based inhibitors (MA-DKA, DA-DKA and L-708,906) and L-chicoric acid.[21,22] HIV susceptibility to some other inhibitors increased in the presence of S153Y.[20] Virus mutated at position S153Y had diminished integration and replicative capacity in cell culture while the addition of T66I partially restored both activities.[22] S153Y also decreased purified recombinant integrase catalytic activities.[20,22] More recently, S153Y was found to emerge during tissue culture selection experiments with cabotegravir,[23,24] dolutegravir[25] and bictegravir.[24] In some cases, S153Y developed first, before being replaced by R263K,[26] which is itself clinically relevant in the context of dolutegravir therapy.[17,18,27] This observation raised the possibility that S153Y and R263K may be incompatible for reasons of either decreased viral replicative capacity or reduced drug resistance levels. By itself, S153Y conferred only low levels of resistance against clinically relevant integrase inhibitors in cell culture.[23,24,28,29] Other rare changes at position 153 that have been found in cell culture include S153F and S153A.[24] Little is known about the effect of S153F/A on HIV integration and replicative capacity.[25] Despite being frequently observed in cell culture, S153Y has never been observed in patients, to the best of our knowledge; S153F has been reported only once.[30,31] We report here the detection by ultradeep sequencing of the S153F integrase substitution in combination with R263K in the proviral DNA of peripheral blood cells from one individual treated with dolutegravir-based therapy. Both deep sequencing and clonal analyses confirmed the coexistence of the two mutations on single genomes. We characterized the effects of the S153F, S153Y and R263K substitutions, alone or in combination, on integrase strand transfer and DNA-binding activities and viral infectivity, replicative capacity and resistance against integrase inhibitors. We confirmed previous observations regarding the S153Y and R263K individual substitutions and showed that combining S153Y/F with R263K further impaired integrase strand transfer activity, viral infectivity and replicative capacity compared with single mutations. The S153Y/F plus R263K combinations of mutations conferred very high levels of resistance against all integrase inhibitors. Altogether, we report that highly resistant viruses can emerge as minority species in successfully ART-treated patients despite being poorly replicative; however, these highly resistant minority variants do not ineluctably drive treatment failure.

Patient and methods

Ethics

Research was conducted in accordance with the Declaration of Helsinki. Ethics approval was obtained from the McGill University Health Centre Biomedical Research Ethics Board (MEDB-97-435).

Patient

PBMCs were obtained from one HIV-positive individual who donated blood in the context of the Montréal HIV Primo Infection Cohort through the Réseau SIDA et Maladies Infectieuses of the Fonds de Recherche du Québec en Santé (FRQ-S). The patient was part of a cohort of 14 individuals who were randomly selected from the Primo Infection Cohort because they were treatment-naive integrase inhibitor users who maintained suppression throughout their monitoring. The patient was diagnosed with an HIV-1 subtype B infection (CD4 T cell count of 720 cells/μL and viral load of 32 800 RNA copies/mL) and initiated ART with dolutegravir, lamivudine and abacavir. After 5 weeks, the patient's viral load was, and remained, undetectable (<40 copies/mL) throughout the monitoring period.

Cells and reagents

DMEM, Roswell Park Memorial Institute (RPMI) medium and FBS for cell culture were purchased from Thermo Fisher (Thermo Fisher Scientific, Montréal, QC, Canada). PM1, human embryonic kidney 293 (HEK-293) and TZM-bl cells were obtained from the NIH AIDS Reagent Program, NIAID, NIH. HEK-293 and TZM-bl cells were grown at 37°C in DMEM supplemented with 10% FBS, 2 mM L-glutamine, 50 U/mL penicillin and 50 μg/mL streptomycin, in the presence of 5% CO_2. PM1 cells were cultured under the same conditions but with RPMI as base medium.

Viruses

The proviral pNL4.3 plasmid that encodes for a replicative HIV-1 subtype B virus was obtained from the NIH AIDS Reagent Program.[32] The same plasmid was previously mutated into pNL4.3$_{R263K}$, which bears the R263K substitution within the integrase coding sequence.[26] The S153F and S153Y substitutions in integrase were added to either pNL4.3 or pNL4.3$_{R263K}$ in order to produce the pNL4.3$_{S153F}$, pNL4.3$_{S153Y}$, pNL4.3$_{S153F/R263K}$ and pNL4.3$_{S153Y/R263K}$ through site-directed mutagenesis (SDM), as previously described.[33] Primers for SDM were: TTCTTTAATTCTTTATTCATAAATTCTATTA CTCCTTGACTTTGGGGATTGTAG (S153F sense), CTACAATCCCCAAAGTCAAGGA GTAATAGAATTTATGAATAAAGAATTAAAGAA (S153F antisense), TTCTTTAA TTCTTTATTCATATATTCTATTACTCCTTGACTTTGGGGATTGTAG (S153Y sense) and CTACAATCCCCAAAGTCAAGGAGTAATAGAATATATGAATAAAGAATTAAAG AA (S153Y antisense). Proper mutagenesis was verified by sequencing. The above-described plasmids were transfected into HEK-293 cells using Lipofectamine 2000 (Thermo Fisher Scientific) in order to produce replication-competent viruses, following a previously described protocol.[34] Viral production was measured through reverse transcriptase (RT) quantification[35] and viral stocks were aliquoted and stored at −80°C.

Ultradeep sequencing

HIV proviral DNA was sequenced using methods described elsewhere.[36] Briefly, nested PCR was used to amplify four DNA fragments covering nearly the entire HIV genome. Each amplicon was amplified twice in separate duplicates and later combined to produce sequencing libraries using a Nextera XT DNA sample preparation kit (version 3, Illumina, San Diego, CA, USA). Library qualities were verified using a Qubit fluorometer (Thermo Fisher Scientific). Ultradeep sequencing runs were performed on a MiSeq sequencer (Illumina). Data analysis was performed as described previously.[36] Resistant variants were identified using the Geneious version 9.1.3 software and a list of pre-defined drug resistance substitutions. To investigate the linkage between the S153F/Y and R263K integrase resistance mutations, paired reads were merged before being reference-mapped.[36] A region covering both positions was selected and unique haplotypes were identified. Variants were defined in relation to the annotated reference and relative frequencies were calculated. All merged reads containing both positions were considered.

Cloning and sequencing

The entire integrase coding sequence was amplified using primer pair INF (5′-CCAGTTAGAGAAAGAACCCATA-3′) and INR (5′-TGAGGGCTTTCA TAGTGATGT-3′). The resulting 1.3 kb PCR product was cloned into a pGEMT-T Easy Vector and single clones were sequenced in both directions using T7 and M13R standard primers.

Strand transfer assay

Cell-free strand transfer assays were performed as described previously.[35,37–40] Briefly, recombinant His-tagged WT or mutant integrase proteins were produced in bacteria and purified using Ni-NTA purification columns. S153F/Y mutations were added to either a WT or R263K-mutated integrase sequence previously cloned within a pET15b expression vector to generate the S153F, S153Y and S153F/R263K and S153Y/R263K mutants via SDM. Primers for SDM were identical to those described above for the production of pNL4.3 mutants. Double-stranded DNA long terminal repeat (LTR) fragments immobilized on DNA-Bind 96-well plates (Thermo Fisher Scientific) served as substrate for the recombinant enzymes to integrate target DNA molecules labelled with biotin. Manganese was used in the reaction buffers instead of magnesium because the former helps to obtain higher *in vitro* readings.[39] Strand transfer reactions were permitted to occur for 1 hour at 37°C. After extensive washes, integrated biotinylated DNA molecules were detected using europium-conjugated streptavidin and time-resolved fluorescence on a FLUOStar Optima plate reader (BMG Labtech). These experiments were performed with various concentrations of either integrase proteins or target DNA. First, serial dilutions of recombinant proteins were tested for strand transfer activity in the presence of 20 nM target DNA. Next, the catalytic activity of 400 nM recombinant proteins was measured with serial dilutions of target DNA. From the latter experiments, maximal strand transfer activity (expressed as V_{max}) and the concentration of target DNA needed to reach half-maximal activity (K_m equivalent) were calculated using the GraphPad Prism version 5.0 software. Ninety-five percent (95%) CIs were also calculated for both values. The V_{max}/K_m ratio was calculated as a measure of overall enzyme efficiency. Importantly, all integration assays were performed with three independent purification batches of integrase enzymes. For each of the three batches, all integrase proteins (WT and mutants) were purified simultaneously. Catalytic parameters were consistent throughout, excluding the possibility of purification-related enzyme inactivation.

Integrase–DNA binding assays

We measured the binding activities of WT and mutant integrase proteins to DNA using previously published methods.[41] Briefly, 400 nM WT or mutant integrase proteins (two different batches purified independently) were immobilized covalently onto 96-well high-bind microplates (Corning, MA, USA) in PBS (pH 7.4). Blocking was performed with 5% BSA diluted in PBS. Rhodamine red (RhoR)-labelled and complementary oligonucleotides were purchased from Integrated DNA Technologies (IDT, IA, USA). Oligonucleotide sequences were: 5′-CTTTTAGTCAGTGTGGAAAATCTCTAGCA GT-3′ and 5′-RhoR-ACTGCTAGAGATTTTCCACACTGACTAAAAG-3′, corresponding to HIV-1 subtype B LTR sequences. Integrase–LTR DNA binding was quantified following the incubation of RhoR DNA duplexes at various (0–500 nM) concentrations with the immobilized integrase proteins for 1 h at room temperature. Following washes, fluorescence was quantified on a FLUOStar Optima plate reader. Apparent K_m values were calculated using the GraphPad Prism version 5.0 software.

Infectivity and resistance assays

To measure viral infectivity, 30 000 TZM-bl reporter cells were infected with serial dilutions of WT or mutant virus in 96-well plates. After 48 h, cell supernatants were removed, cells were lysed and luciferase production was measured using a Luciferase Assay System (Promega, Madison, WI, USA). Three wells were used for each viral concentration and two independent experiments were performed. Raw data from these two independent experiments were plotted together without any additional treatment. Arbitrary relative luminescence units (RLUs) were plotted against a logarithmic transformation of viral concentrations expressed in RT activity using the GraphPad Prism version 5.0 software. Relative EC_{50} values and 95% CIs were calculated as a measure of relative infectivity. Resistance assays were performed using 30 000 TZM-bl cells infected with volumes of WT and mutant virus amounting to 30 000 RT units. Serial dilutions of integrase inhibitor were added at the time of infection. After 48 h, luciferase production was measured as described above. These experiments were performed at least three times independently, in triplicates. Luminescence units were plotted against a logarithmic transformation of drug concentrations expressed as nM. GraphPad Prism was used to calculate IC_{50} values and 95% CIs. Fold changes in resistance levels were expressed relative to the IC_{50} of each drug with the WT virus.

Replication assay

To measure HIV replicative capacity, PM1 cells were infected with viral amounts equivalent to 30 000 RT units. After washes, viral growth was monitored over time every 3 days for 17 days by quantifying viral RT activity in cell culture fluids. Uninfected cells were added every 3 days following media removal.

In silico structural modelling

Protein Data Bank (PDB) coordinates of the recently released 5U1C cryogenic electron microscopic structure of HIV integrase was downloaded from the PDB database.[42] Visualization, analysis and modifications were performed in PyMOL version 2.3.2 (Shrodinger LLC). In order to identify potential disruptions caused by mutations, residues being probed were mutated using the mutation wizard in PyMOL. In each case, potential sidechain interactions were measured and compared with those of the WT. For 153Y and 153 F, the two best sidechain rotamers were evaluated for altered interactions relative to WT integrase using previous methods.[43] The two best rotamers were determined to be those with the lowest energy conformations, based on the Dunbrack backbone-dependent rotamer library.[44]

Results

Presence of the S153F and R263K substitutions in HIV proviral DNA from one individual

We report the detection of mutations at integrase positions S153F and R263K in the proviral DNA from the PBMCs of one patient (Table 1). No mutation was found at Week 4. R263K was first detected in 16.3% of the viral population after 8 weeks of treatment, followed by S153F (32.9%) at Week 12, and both substitutions persisted from Weeks 12 to 24. To test whether S153F and R263K coexisted in single genomes, we quantified their linkage in ultradeep sequencing merged reads (Table 2). At 12 weeks, when the two substitutions were first detected concomitantly, 18% of sequences carried both mutations on single genomes. This frequency decayed at Week 24, when only 1.41% of reads carried both S153F and R263K. No other resistance mutation was found in the *pol* gene. Near full-length sequencing was performed as previously published[36] and showed no additional mutation (>10%) in other genes (via NCBI Blast), nor in the 3′ polypurine tract, which is suspected to contribute to resistance to integrase

Table 1. R263K and S153F codon change, coverage and variant frequency at Weeks 8, 12 and 24

Visit	Substitution	Codon change	Coverage (reads)	Variant frequency (%)
Week 8	R263K	AGA to AAA	89 842	16.3
	S153F	—	—	0.0
Week 12	R263K	AGA to AAA	87 301	31.5
	S153F	TCT to TTT	81 294	32.9
Week 24	R263K	AGA to AAA	55 110	24.8
	S153F	TCT to TTT	55 006	6.4

2% cut-off.

Table 2. Number of reads, coverage and frequency of linkage of S153F with substitutions at position 263 at Weeks 8, 12 and 24

Visit	Extracted sequences (merged reads)	Substitution	Coverage (merged reads)	Linkage frequency (%)
Week 8	3740	S153F only	0	—
		S153F and R263K	0	—
		S153F and R263 (non-R/K)	0	—
Week 12	4688	S153F only	7	0.15
		S153F and R263K	842	18
		S153F and R263 (non-R/K)	3	—
Week 24	1270	S153F only	12	0.94
		S153F and R263K	18	1.41
		S153F and R263 (non-R/K)	1	—

inhibitors.[17,45–47] From Week 24, we cloned amplicons covering the two positions into a pGEM-T Easy Vector. From 27 clonal sequences, one (3.4%) contained both mutations simultaneously (data not shown). These results showed that viruses with both S153F and R263K could exist in the proviral DNA.

Combining S153F/Y with R263K reduces integrase strand transfer activity

Since we found the S153F/R263K combination of substitutions to emerge *in vivo*, and given the frequent cell-based selection of the S153Y substitution, we characterized the effects of the S153F/Y plus R263K combinations of substitutions on integrase strand transfer activity (Figure 1). All recombinant proteins yielded the highest strand transfer activity at 400 nM. The catalytic activities of mutants were reduced compared with WT integrase. In order to dynamically analyse the strand transfer activity of each mutant, strand transfer assays were performed in the presence of various concentrations (0–480 nM) of target DNA substrate (Figure 2a). These experiments confirmed the deleterious effects of individual substitutions on integration while providing detailed information regarding changes in integrase enzymatic activity. Maximal integration activities of S153F, S153Y and S153Y/R263K mutated integrase proteins were comparable and higher than that of the S153F/R263K double mutant (Figure 2b). The addition of S153F/Y to R263K decreased apparent integrase affinity for the target DNA substrate (as estimated by equivalent K_m values; Table 3). However, when S153F by itself was less detrimental to integrase–DNA binding than S153Y, the S153F/R263K combination had a more profound negative effect on this activity than S153Y/R263K. As a result, the overall efficiency of the S153F/R263K enzyme was the lowest of all mutants (Table 3). In addition, integrase–DNA binding activities were directly measured for all proteins (Table 3). These experiments confirmed that the double mutant S153F/R263K and S153Y/R263K proteins had reduced DNA-binding affinities (by 10.4- and 2.4-fold, respectively).

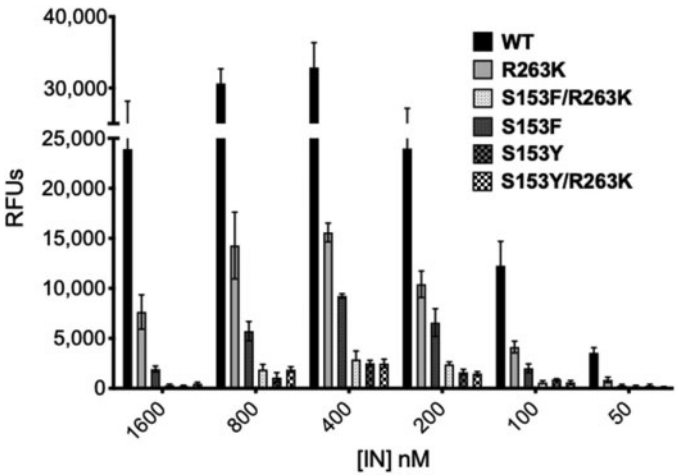

Figure 1. Strand transfer activity, in relative fluorescence units (RFUs), of various concentrations of WT and mutant integrase (IN) proteins.

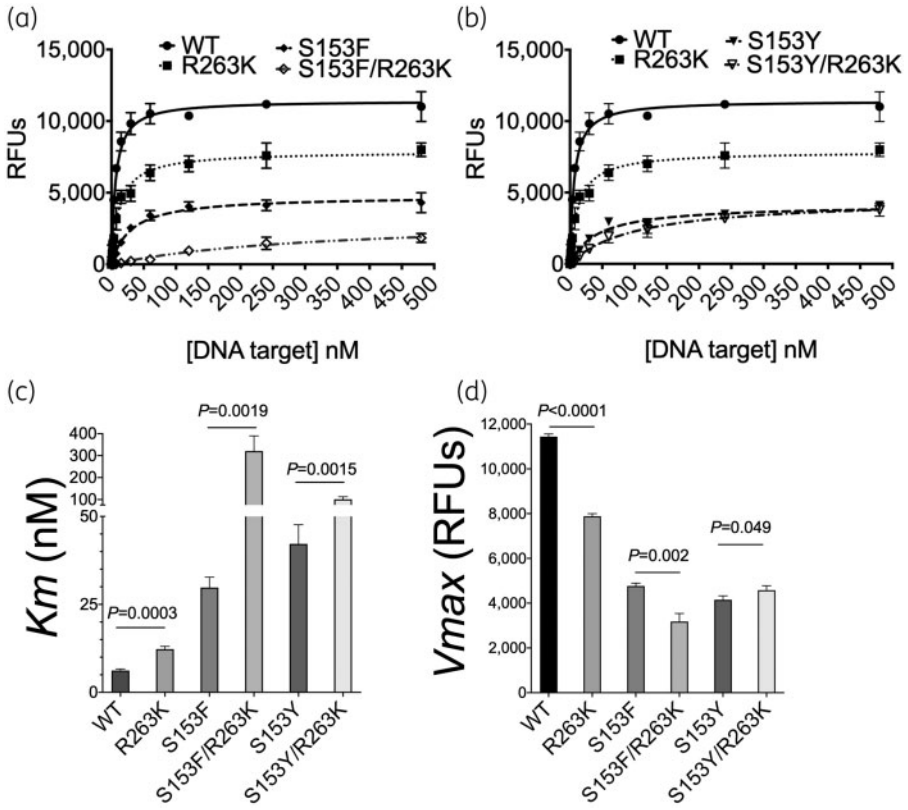

Figure 2. (a) Strand transfer activity, in relative fluorescence units (RFUs), of WT and mutant integrase proteins in the presence of various concentrations of target DNA. (b) Apparent K_m (half-maximal DNA) and maximum catalytic activity (V_{max}) values.

Table 3. Catalytic parameters of purified recombinant WT and mutant integrase proteins

	Strand transfer assay parameters			Integrase–DNA binding assay
Enzyme	V_{max} (95% CI)	apparent K_m (95% CI)	V_{max}/K_m ratio	K_m (95% CI)
WT	11 439 (11 086–11 792)	6.2 (5.3–7.1)	1845	22.01 (15.34–28.7)
R263K	**7878[a] (7640–8116)**	**12.27[a] (10.68–13.85)**	642	25.02 (17.79–32.25)
S153F	**4766[a] (4504–5027)**	**29.79[a] (23.83–35.76)**	160	29.8 (22.1–37.5)
S153F/R263K	**3177[a,b] (2449–3904)**	**320.9[a,b] (182.3–459.5)**	10	**229.8[a,b] (78.25–381.4)**
S153Y	4149 (3796–4503)	**42.19[a] (31.26–53.12)**	98	27.08 (15.04–39.12)
S153Y/R263K	**4579[a,b] (4176–4981)**	**101.90[a,b] (76.99–125.1)**	45	**53.1[a] (29.1–77.1)**

Bold text indicates statistical significance.
[a]Statistically significant compared with WT.
[b]Statistically significant compared with single mutant R263K.

Combining S153F/Y with R263K reduces viral infectivity

Next, we tested the effects of S153F/Y and R263K on HIV-1 subtype B short-term infectivity (Figure 3). Infectivity curves showed that S153F, but not S153Y, had significantly lower infectivity than WT and R263K viruses (Figure 3a). Consistent with results from the strand transfer assays, the S153F/R263K combination of substitution was more detrimental to HIV-1 infectivity than S153Y/R263K, yielding almost 50-fold reduction in half-effective virus concentration versus 16-fold for the latter (Figure 3b).

Combining S153F/Y with R263K reduces HIV-1 replicative capacity

Short-term infectivity assays do not fully recapitulate the ability of a virus to replicate. We thus tested the effects of S153F/Y and R263K integrase substitutions on HIV-1 replication over 17 days (Figure 4). Results confirmed our previous studies showing that R263K modestly diminishes HIV-1 replicative capacity.[26,48] S153Y similarly reduces the replication peak by about 2-fold. In contrast, replicative capacities of the S153F, S153F/R263K and S153Y/R263K viruses were significantly reduced.

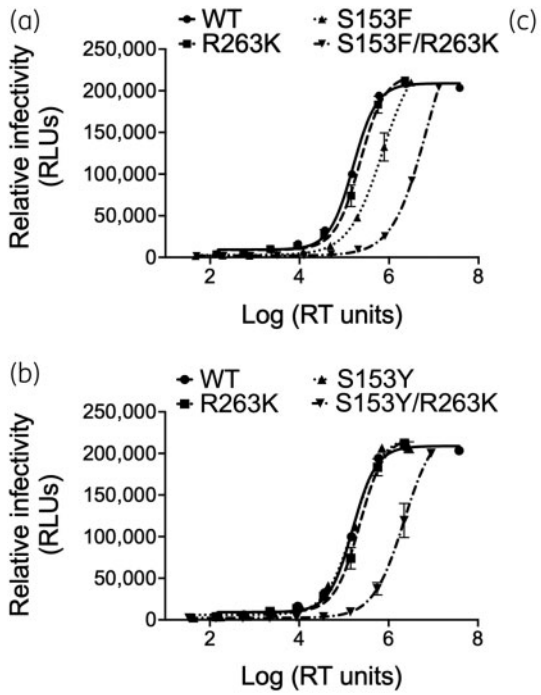

(c)

Genotype	Relative infectivity [95% CI]
WT	1 [0.92-1.09]
R263K	1.36[a] [1.19-1.59]
S153F	4.94[a] [4.12-6.4]
S153F/R263K	48.1[a,b] [41.95-56.9]
S153Y	1.31[a] [1.17-1.48]
S153Y/R263K	15.94[a,b] [13.09-21.8]

[a]Statistically different from WT

[b]Statistically superior to S153F

Figure 3. (a, b) Infectivity curves of the WT and mutant viruses. (c) Relative infectivity and 95% CIs for the WT and mutant viruses in cell culture.

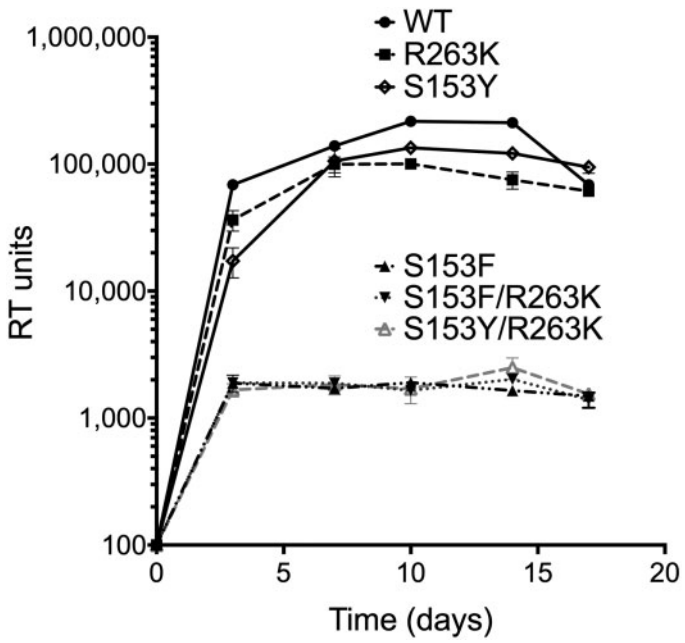

Figure 4. Replicative capacity in cell culture of WT and mutant viruses over 17 days.

S153F/Y plus R263K combinations of substitutions are associated with high levels of drug resistance

Drug resistance assays confirmed previous reports from others and us showing that R263K conferred low levels of resistance against dolutegravir and bictegravir (Table 4).[26,29,48] S153F alone conferred 7.94-fold resistance against bictegravir but remained fully susceptible to dolutegravir and raltegravir. This substitution was also highly susceptible to cabotegravir. By itself, S153Y had minor effects on HIV-1 susceptibility to raltegravir (3.29-fold change) and bictegravir (2.21-fold change), in agreement with previous reports.[25,29] Dolutegravir and cabotegravir were as efficacious against the S153Y mutant as against the WT virus. The S153F/Y plus R263K double mutants were highly resistant against all INSTIs tested.

In silico structure modelling of S153F/Y and R263K integrase proteins

Both R263 and S153 interact directly with opposing strands of the double-stranded viral DNA (Figure 5a). R263 contacts the viral strand that becomes covalently linked to the host DNA during integration whereas S153 interacts with the opposing DNA strand. The highly basic guanidino group of the R263 sidechain stabilizes the strand transfer complex (Figure 5b) by forming multiple electrostatic interactions with the viral DNA and two residues of the integrase active site loop (N144 and Q146). In contrast, K263 is less basic and cannot establish all those electrostatic interactions (Figure 5c), which means that synaptic complexes are less stable. This translates into suboptimal DNA binding, diminished catalytic activity and resistance against some inhibitors.[26,49] S153 is in direct hydrogen-bonding contact with viral DNA (Figure 5d), whereas S153Y/F substitutions create a steric hindrance that may affect the conformation of integrase alpha helix 8 (residues 148–166), the viral DNA or both (Figure 5e). Backbone changes in alpha helix 8 can affect the sidechain orientation of the catalytic residue E152 relative to the other two residues of the catalytic triad, thereby impacting catalytic activity and drug resistance.

Table 4. Phenotypic susceptibility of WT and mutant viruses to dolutegravir (DTG), bictegravir (BIC), cabotegravir (CAB), raltegravir (RAL) and elvitegravir (EVG) in cell culture

Genotype	DTG fold resistance (95% CI)	BIC fold resistance (95% CI)	CAB fold resistance (95% CI)	RAL fold resistance (95% CI)	EVG fold resistance (95% CI)
WT	1 (0.7–1.48)	1 (0.74–1.37)	1 (0.9–1.1)	1 (0.93–1.07)	1 (0.6–1.7)
R263K	**2.28[a] (1.6–3.2)**	**7.36[a] (3.9–14.6)**	1.2 (0.8–1.6)	1.27 (1.15–1.4)	2.17 (0.2–14.4)
S153F	0.5 (0.3–0.9)	**7.94[a] (4.7–13.6)**	H.S.	0.44 (0.17–1.2)	4.62 (1.4–10.5)
S153Y	1.1 (0.9–1.4)	**2.21[a] (1.5–3.1)**	1.34 (1.1–1.6)	**3.29[a] (2.2–6.1)**	2.14 (1–3.6)
S153F/R263K	**>100**	**>100**	**>100**	**>100**	**>100**
S153Y/R263K	**>100**	**>100**	**>100**	**>100**	**>100**

H.S., hypersusceptibility.
[a]Statistically significant compared with WT.

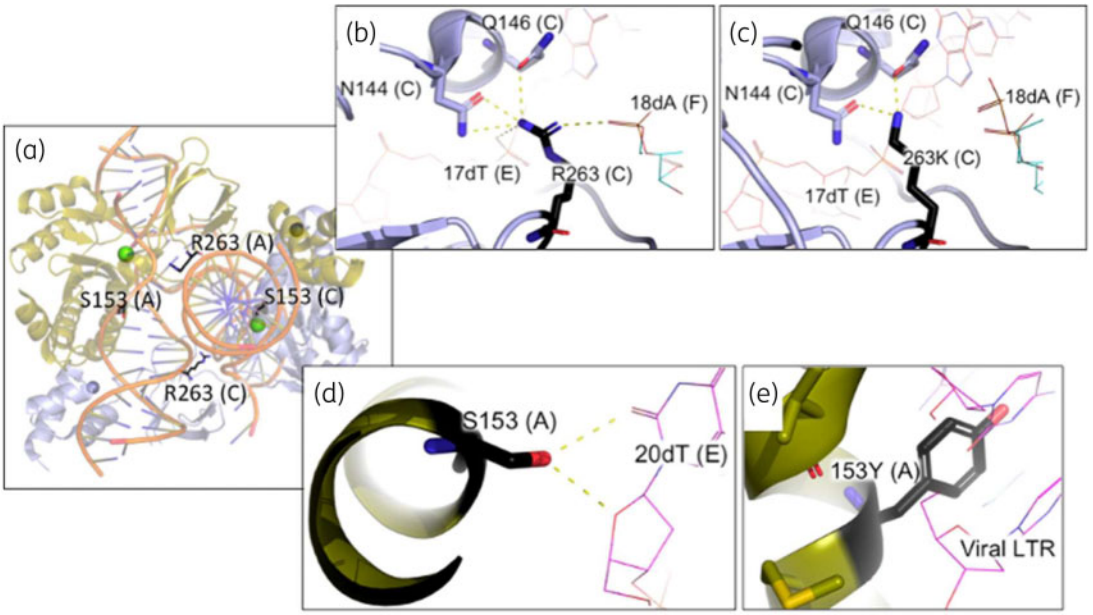

Figure 5. *In silico* structure modelling of the HIV-1 integrase/DNA nucleoprotein complex. (a) Overall view showing the S153 and R263 residues interacting with opposite viral DNA strands. (b) Detailed electrostatic interactions of R263 with both the viral DNA and residues of the integrase active site loop (N144 and Q146). (c) Detailed electrostatic interactions of 263K with N144 and Q146. (d) Hydrogen-bonding contacts between S153 and HIV-1 DNA. (e) Steric hindrance between 153Y and the viral DNA. Similar results were obtained for 153F. This figure appears in colour in the online version of JAC and in black and white in the print version of JAC.

Discussion

We report here the identification of the S153F/R263K combination of substitutions in one patient successfully treated with a dolutegravir-based antiretroviral drug regimen. Our detailed characterization of the S153F, S153Y and R263K substitutions alone or in combination provides potential explanations for the rarity of these mutations in patients. Cell-free strand transfer and infectivity assays overall demonstrated that combining S153F/Y with R263K negatively affects integration and viral infectivity (Table 3 and Figure 3). Most of these defects stem from decreases in DNA binding that are observed both *in vitro* and in *in silico* structural modelling where R263 and S153 each act on opposite viral DNA strands to stabilize the nucleoprotein complex structure (Table 3 and Figure 5). Notably, these results also help to explain the high levels of resistance associated with the double mutants in cell culture. Indeed, optimal binding of integrase inhibitors to the integrase catalytic site depends on conformational changes induced by DNA binding and base stacking of integrase inhibitors with DNA. Decreasing DNA binding would thus disfavour the binding of inhibitors. Others have also used molecular modelling to explain resistance against various integrase inhibitors, highlighting the usefulness of this approach to better understand viral protein variability, resistance and compensation mechanisms.[49–52] The R263K substitution induces similar changes in DNA binding that are also associated with resistance against dolutegravir.[26,53] This reciprocally also diminishes integration *in vitro* and HIV-1 infectivity[26] (see Figures 2 and 3). Accordingly, short-term replication assays

indicated that the S153F/R263K and S153Y/R263K combinations of substitutions reduced HIV-1's ability to replicate (Figure 4). This last observation also helps to explain why S153F/R263K double mutants existed only transiently in this patient, peaking at about 20% of the viral population at Week 12 before decreasing below 2% at Week 24, despite high levels of drug resistance (Table 2). There is evidence that viruses carrying either S153F or R263K can replicate *in vivo*.[18,31,54] Longitudinal sequencing results indicated that R263K emerged first followed by S153F (Table 1). This observation is consistent with the resistance profiles of S153F and R263K mutant viruses. Indeed, S153F by itself did not decrease susceptibility to dolutegravir (Table 4). It is thus unlikely to emerge first under dolutegravir pressure. Although S153F seemed to be marginally more frequent than R263K at Week 12 (32.9% versus 31.5%, respectively; Table 1), the small percentage difference between the two substitutions was below 2% and did not permit us to conclude that S153F evolved independently. The conclusion that S153F is unlikely to have emerged separately was also supported by linkage analysis, showing S153F by itself in <2% of sequences (0.15% at Week 12 and 0.94% at Week 24; Table 2). Since viral suppression in plasma was maintained throughout, we assume that the S153F and R263K combination either spontaneously emerged from reservoirs or that they were produced by recombination. Sequences were, in the majority, without premature stop codons and there were no stop codons in the reads that contained both S153F and R263K. Together with the maintenance of viral suppression over the 24 week observation period, our study demonstrates that the occurrence of rare, poorly replicative highly resistant strains in the proviral DNA does not unavoidably lead to virological failure under dolutegravir-based HAART. Why such resistant variants were not detected in patients who have been reported as failing such treatment is a question that remains unanswered. Together with the recent involvement of proviral mutations in failure with long-acting cabotegravir plus rilpivirine, our report also raises the question of whether our patient would benefit from this new antiretroviral regimen.[55,56]

Acknowledgements

This work was made possible thanks to access to clinical samples obtained through the Fonds de Recherche du Québec en Santé – Réseau SIDA et Maladies Infectieuses. We thank the following for supplying reagents through the NIH Reagents Program: Marvin Reiz (PM1); Andrew Rice (HEK-293); and John C. Kappes and Xiaoyun Wu (TZM-bl). We thank Malcolm Martin of the NIH AIDS Reagent Program for the proviral pNL4.3 plasmid. We are grateful to our research coordinators (Mario Legaux and Olfa Debbeche) and to the participant for their generous blood donations.

Funding

This study was supported by internal funding.

Transparency declarations

None to declare.

References

1 Saag MS, Benson CA, Gandhi RT *et al.* Antiretroviral drugs for treatment and prevention of HIV infection in adults: 2018 recommendations of the International Antiviral Society-USA Panel. *JAMA* 2018; **320**: 379–96.

2 Mesplede T, Quashie PK, Zanichelli V *et al.* Integrase strand transfer inhibitors in the management of HIV-positive individuals. *Ann Med* 2014; **46**: 123–9.

3 Pham HT, Mesplede T. Bictegravir in a fixed-dose tablet with emtricitabine and tenofovir alafenamide for the treatment of HIV infection: pharmacology and clinical implications. *Expert Opin Pharmacother* 2019; **20**: 385–97.

4 Wainberg MA, Zaharatos GJ, Brenner BG. Development of antiretroviral drug resistance. *N Engl J Med* 2011; **365**: 637–46.

5 Anstett K, Brenner B, Mesplede T *et al.* HIV drug resistance against strand transfer integrase inhibitors. *Retrovirology* 2017; **14**: 36.

6 Mesplede T, Wainberg MA. Resistance against integrase strand transfer inhibitors and relevance to HIV persistence. *Viruses* 2015; **7**: 3703–18.

7 Rhee SY, Grant PM, Tzou PL *et al.* A systematic review of the genetic mechanisms of dolutegravir resistance. *J Antimicrob Chemother* 2019; **74**: 3135–49.

8 Brenner BG, Thomas R, Blanco JL *et al.* Development of a G118R mutation in HIV-1 integrase following a switch to dolutegravir monotherapy leading to cross-resistance to integrase inhibitors. *J Antimicrob Chemother* 2016; **71**: 1948–53.

9 Gubavu C, Prazuck T, Niang M *et al.* Dolutegravir-based monotherapy or dual therapy maintains a high proportion of viral suppression even in highly experienced HIV-1-infected patients. *J Antimicrob Chemother* 2016; **71**: 1046–50.

10 Katlama C, Soulie C, Caby F *et al.* Dolutegravir as monotherapy in HIV-1-infected individuals with suppressed HIV viraemia. *J Antimicrob Chemother* 2016; **71**: 2646–50.

11 Lanzafame M, Gibellini D, Lattuada E *et al.* Dolutegravir monotherapy in HIV-infected naive patients with <100 000 copies/mL HIV RNA load. *J Acquir Immune Defic Syndr* 2016; **72**: e12–4.

12 Moreira J. Dolutegravir monotherapy as a simplified strategy in virologically suppressed HIV-1-infected patients. *J Antimicrob Chemother* 2016; **71**: 2675–6.

13 Oldenbuettel C, Wolf E, Ritter A *et al.* Dolutegravir monotherapy as treatment de-escalation in HIV-infected adults with virological control: DoluMono cohort results. *Antivir Ther* 2017; **22**: 169–72.

14 Rojas J, Blanco JL, Marcos MA *et al.* Dolutegravir monotherapy in HIV-infected patients with sustained viral suppression. *J Antimicrob Chemother* 2016; **71**: 1975–81.

15 Rokx C, Schurink CA, Boucher CA *et al.* Dolutegravir as maintenance monotherapy: first experiences in HIV-1 patients. *J Antimicrob Chemother* 2016; **71**: 1632–6.

16 Wijting I, Rokx C, Boucher C *et al.* Dolutegravir as maintenance monotherapy for HIV (DOMONO): a phase 2, randomised non-inferiority trial. *Lancet HIV* 2017; **4**: e547–54.

17 Wijting IEA, Lungu C, Rijnders BJA *et al.* HIV-1 resistance dynamics in patients with virologic failure to dolutegravir maintenance monotherapy. *J Infect Dis* 2018; **218**: 688–97.

18 Cahn P, Pozniak AL, Mingrone H *et al.* Dolutegravir versus raltegravir in antiretroviral-experienced, integrase-inhibitor-naive adults with HIV: week 48 results from the randomised, double-blind, non-inferiority SAILING study. *Lancet* 2013; **382**: 700–8.

19 Hazuda DJ, Felock P, Witmer M *et al.* Inhibitors of strand transfer that prevent integration and inhibit HIV-1 replication in cells. *Science* 2000; **287**: 646–50.

20 Zahm JA, Bera S, Pandey KK *et al*. Mechanisms of human immunodeficiency virus type 1 concerted integration related to strand transfer inhibition and drug resistance. *Antimicrob Agents Chemother* 2008; **52**: 3358–68.

21 Svarovskaia ES, Barr R, Zhang X *et al*. Azido-containing diketo acid derivatives inhibit human immunodeficiency virus type 1 integrase in vivo and influence the frequency of deletions at two-long-terminal-repeat-circle junctions. *J Virol* 2004; **78**: 3210–22.

22 Lee DJ, Robinson WE Jr. Human immunodeficiency virus type 1 (HIV-1) integrase: resistance to diketo acid integrase inhibitors impairs HIV-1 replication and integration and confers cross-resistance to L-chicoric acid. *J Virol* 2004; **78**: 5835–47.

23 Yoshinaga T, Kobayashi M, Seki T *et al*. Antiviral characteristics of GSK1265744, an HIV integrase inhibitor dosed orally or by long-acting injection. *Antimicrob Agents Chemother* 2015; **59**: 397–406.

24 Oliveira M, Ibanescu RI, Anstett K *et al*. Selective resistance profiles emerging in patient-derived clinical isolates with cabotegravir, bictegravir, dolutegravir, and elvitegravir. *Retrovirology* 2018; **15**: 56.

25 Kobayashi M, Yoshinaga T, Seki T *et al*. In vitro antiretroviral properties of S/GSK1349572, a next-generation HIV integrase inhibitor. *Antimicrob Agents Chemother* 2011; **55**: 813–21.

26 Quashie PK, Mesplede T, Han YS *et al*. Characterization of the R263K mutation in HIV-1 integrase that confers low-level resistance to the second-generation integrase strand transfer inhibitor dolutegravir. *J Virol* 2012; **86**: 2696–705.

27 Taiwo BO, Zheng L, Stefanescu A *et al*. ACTG A5353: a pilot study of dolutegravir plus lamivudine for initial treatment of human immunodeficiency virus-1 (HIV-1)-infected participants with HIV-1 RNA <500000 copies/mL. *Clin Infect Dis* 2018; **66**: 1689–97.

28 Kobayashi M, Nakahara K, Seki T *et al*. Selection of diverse and clinically relevant integrase inhibitor-resistant human immunodeficiency virus type 1 mutants. *Antiviral Res* 2008; **80**: 213–22.

29 Smith SJ, Zhao XZ, Burke TR Jr *et al*. Efficacies of cabotegravir and bictegravir against drug-resistant HIV-1 integrase mutants. *Retrovirology* 2018; **15**: 37.

30 Garrido C, Soriano V, Geretti AM *et al*. Resistance associated mutations to dolutegravir (S/GSK1349572) in HIV-infected patients—impact of HIV subtypes and prior raltegravir experience. *Antiviral Res* 2011; **90**: 164–7.

31 Malet I, Wirden M, Fourati S *et al*. Prevalence of resistance mutations related to integrase inhibitor S/GSK1349572 in HIV-1 subtype B raltegravir-naive and -treated patients. *J Antimicrob Chemother* 2011; **66**: 1481–3.

32 Adachi A, Gendelman HE, Koenig S *et al*. Production of acquired immunodeficiency syndrome-associated retrovirus in human and nonhuman cells transfected with an infectious molecular clone. *J Virol* 1986; **59**: 284–91.

33 Pham HT, Mesplede T, Wainberg MA. Effect on HIV-1 viral replication capacity of DTG-resistance mutations in NRTI/NNRTI resistant viruses. *Retrovirology* 2016; **13**: 31.

34 Mesplede T, Leng J, Pham HT *et al*. The R263K dolutegravir resistance-associated substitution progressively decreases HIV-1 integration. *mBio* 2017; **8**: 157–63.

35 Pham HT, Labrie L, Wijting IEA *et al*. The S230R integrase substitution associated with virus load rebound during dolutegravir monotherapy confers low-level resistance to integrase strand-transfer inhibitors. *J Infect Dis* 2018; **218**: 698–706.

36 Alves BM, Siqueira JD, Garrido MM *et al*. Characterization of HIV-1 near full-length proviral genome quasispecies from patients with undetectable viral load undergoing first-line HAART therapy. *Viruses* 2017; **9**: 392–411.

37 Wares M, Mesplede T, Quashie PK *et al*. The M50I polymorphic substitution in association with the R263K mutation in HIV-1 subtype B integrase increases drug resistance but does not restore viral replicative fitness. *Retrovirology* 2014; **11**: 7–14.

38 Mesplede T, Quashie PK, Hassounah S *et al*. The R263K substitution in HIV-1 subtype C is more deleterious for integrase enzymatic function and viral replication than in subtype B. *AIDS* 2015; **29**: 1459–66.

39 Quashie PK, Oliviera M, Veres T *et al*. Differential effects of the G118R, H51Y, and E138K resistance substitutions in different subtypes of HIV integrase. *J Virol* 2015; **89**: 3163–75.

40 Anstett K, Cutillas V, Fusco R *et al*. Polymorphic substitution E157Q in HIV-1 integrase increases R263K-mediated dolutegravir resistance and decreases DNA binding activity. *J Antimicrob Chemother* 2016; **71**: 2083–8.

41 Han YS, Xiao WL, Quashie PK *et al*. Development of a fluorescence-based HIV-1 integrase DNA binding assay for identification of novel HIV-1 integrase inhibitors. *Antiviral Res* 2013; **98**: 441–8.

42 Passos DO, Li M, Yang R *et al*. Cryo-EM structures and atomic model of the HIV-1 strand transfer complex intasome. *Science* 2017; **355**: 89–92.

43 Dunbrack RL Jr, Karplus M. Conformational analysis of the backbone-dependent rotamer preferences of protein sidechains. *Nat Struct Mol Biol* 1994; **1**: 334–40.

44 Dunbrack RL Jr, Karplus M. Backbone-dependent rotamer library for proteins. Application to side-chain prediction. *J Mol Biol* 1993; **230**: 543–74.

45 Malet I, Subra F, Charpentier C *et al*. Mutations located outside the integrase gene can confer resistance to HIV-1 integrase strand transfer inhibitors. *mBio* 2017; **8**: e00922-17.

46 Malet I, Subra F, Richetta C *et al*. Reply to Das and Berkhout, "How polypurine tract changes in the HIV-1 RNA genome can cause resistance against the integrase inhibitor dolutegravir". *mBio* 2018; **9**: e00623-18.

47 Das AT, Berkhout B. How polypurine tract changes in the HIV-1 RNA genome can cause resistance against the integrase inhibitor dolutegravir. *mBio* 2018; **9**: e00006-18.

48 Mesplede T, Quashie PK, Osman N *et al*. Viral fitness cost prevents HIV-1 from evading dolutegravir drug pressure. *Retrovirology* 2013; **10**: 22–8.

49 Cook NJ, Li W, Berta D *et al*. Structural basis of second-generation HIV integrase inhibitor action and viral resistance. *Science* 2020; **367**: 806–10.

50 Machado LA, Gomes M, Guimaraes ACR. Raltegravir-induced adaptations of the HIV-1 integrase: analysis of structure, variability, and mutation co-occurrence. *Front Microbiol* 2019; **10**: 1981.

51 Passos DO, Li M, Jozwik IK *et al*. Structural basis for strand-transfer inhibitor binding to HIV intasomes. *Science* 2020; **367**: 810–4.

52 Engelman AN, Cherepanov P. Close-up: HIV/SIV intasome structures shed new light on integrase inhibitor binding and viral escape mechanisms. *FEBS J* 2020; doi:10.1111/febs15438.

53 Mesplede T, Osman N, Wares M *et al*. Addition of E138K to R263K in HIV integrase increases resistance to dolutegravir, but fails to restore activity of the HIV integrase enzyme and viral replication capacity. *J Antimicrob Chemother* 2014; **69**: 2733–40.

54 Gantner P, Lee GQ, Rey D *et al*. Dolutegravir reshapes the genetic diversity of HIV-1 reservoirs. *J Antimicrob Chemother* 2018; **73**: 1045–53.

55 Orkin C, Arasteh K, Gorgolas Hernandez-Mora M *et al*. Long-acting cabotegravir and rilpivirine after oral induction for HIV-1 infection. *N Engl J Med* 2020; **382**: 1124–35.

56 Hassounah SA, Mesplede T. Where are we with injectables against HIV infection and what are the remaining challenges? *Expert Rev Anti Infect Ther* 2018; **16**: 143–52.